WEP Warwick Evans Publishing

International Journal of Mechanical and Electrical Engineering

ISSN: 3005-9615 (Print), ISSN: 3005-7132 (Online) | Volume 8, Number 3, Year 2026
DOI: https://doi.org/10.62051/ijmee.v8n3.02
Journal homepage: https://wepub.org/index.php/IJMEE/index

Research on PMSM Speed Control based on Active Disturbance Rejection Control

Peng Wang, Xia He and Haojie Liao

School of Mechatronic Engineering, Energy Equipment Institute, Southwest Petroleum University, Chengdu, Sichuan, 610500, China

ABSTRACT

In current permanent magnet synchronous motor (PMSM) control systems,the traditional PI algorithm is commonly employed for motor control and regulation.However,this approach suffers from issues such as prolonged settling time and excessive overshoot.To address these problems,a PMSM control design based on Active Disturbance Rejection Control (ADRC) is proposed.Furthermore,to enhance the motor's operational stability,disturbance rejection capability,and reduce control costs, three speed control strategies for PMSMs are designed based on Nonlinear Active Disturbance Rejection Control (NLADRC),Linear Active Disturbance Rejection Control (LADRC), and PI controllers.By constructing simulation models and conducting simulation experiments,it is demonstrated that,compared to the traditional PI algorithm and LADRC,the NLADRC-based strategy achieves a smoother speed curve,shorter settling time,and smaller overshoot,exhibiting superior real-time performance and robustness.This meets the requirements of industrial control applications,verifying that the NLADRC-based control strategy designed in this paper offers optimal motor response and tracking characteristics.The nonlinear active disturbance rejection control technology successfully enables closed-loop speed control of permanent magnet synchronous motors.

KEYWORDS

PI Controller; ADRC; NLADRC; Real-time Performance; Robustness.

1. INTRODUCTION

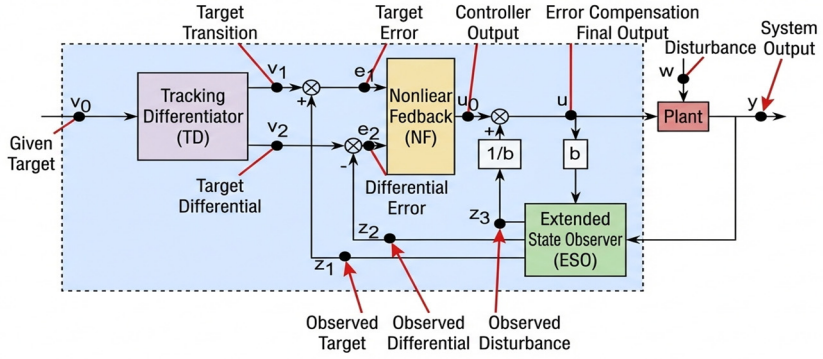

Fig 1. Block Diagram of Second-Order Active Disturbance Rejection Controller Structure

Taking the speed control loop of a Permanent Magnet Synchronous Motor (PMSM) as an example,this section introduces the key components of first-order Nonlinear Active Disturbance Rejection Control

(NLADRC) and their design methods [1][2]. First-order NLADRC mainly consists of three modules: the Tracking Differentiator (TD), the Extended State Observer (ESO), and the Nonlinear State Error Feedback (NLSEF) control law[3]. Fig.1 illustrates the corresponding first-order NLADRC speed loop control structure.

2. RESEARCH ON PMSM SPEED CONTROL BASED ON ACTIVE DISTURBANCE REJECTION CONTROL

2.1. Analysis of Nonlinear Functions

The most renowned and commonly used nonlinear function in ADRC is the fal function (which features a linear region near the origin and a power function further away).The mathematical expression of the fal function adopted in this paper is as follows:

$$fal(e,\alpha,\delta)=\begin{cases}\dfrac{e}{\delta^{1-\alpha}}, |e|\le\delta \\ |e|^{\alpha}\, sgn(e), |e|>\delta\end{cases} \tag{1}$$

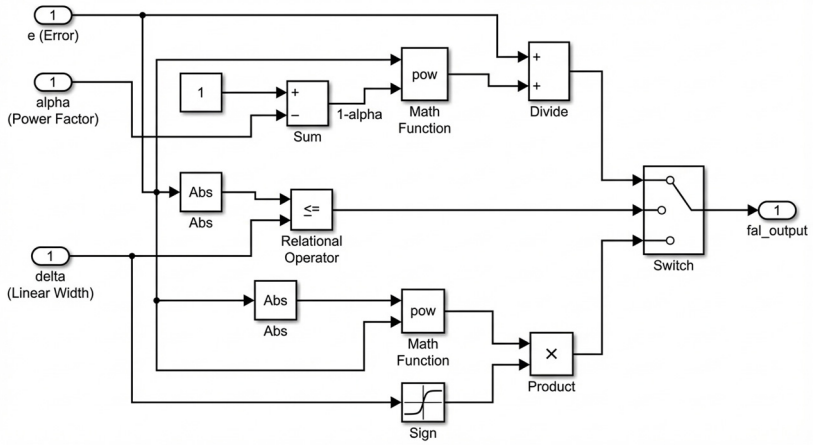

Fig 2. $fal(e,\alpha,\delta)$ Block Diagram of Function Calculation

When δ=0.01 ,taking α=0, 0.25, 0.5,1 respectively,the function images are shown in Fig.3.When α=0.5 ,taking δ=0,0.25,0.5,1 respectively,the function images are shown in Figure 10[4].

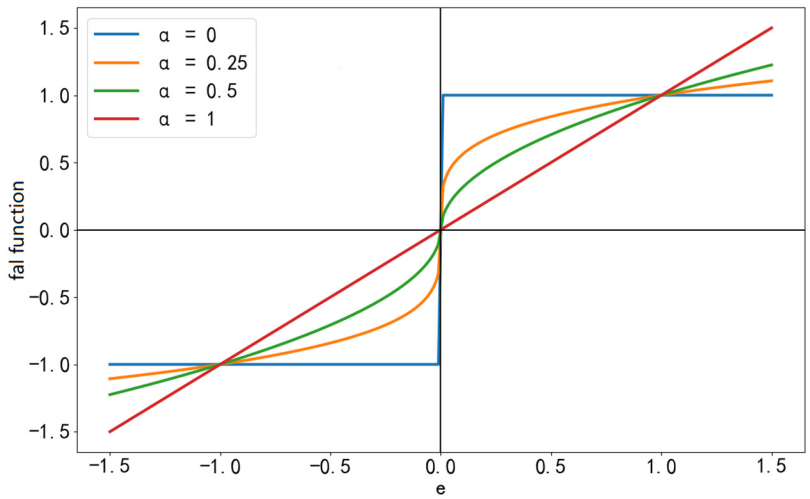

Fig 3. α Function Images of fal for Different Parameter Values

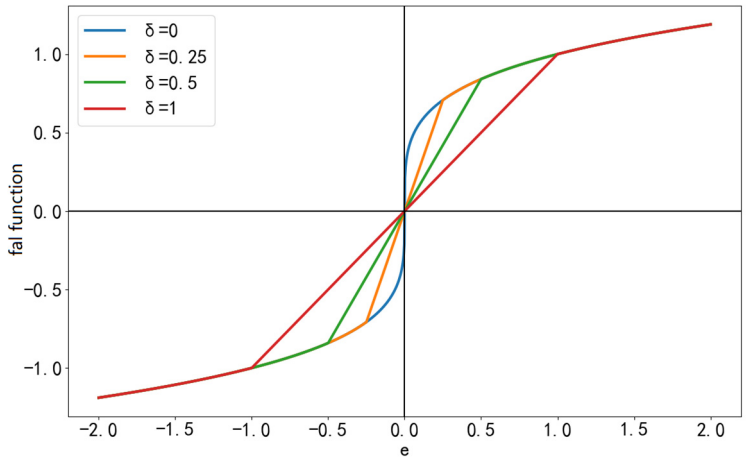

Fig 4. δ Function Images of fal for Different Parameter Values

The fal function is the core component enabling ADRC to achieve the characteristic of small gain for large errors (preventing overshoot) and large gain for small errors (eliminating steady-state error).From the simulation results shown in Figures 3 and 4 above, it can be observed that its performance depends on the trade-off between two parameters: α and δ .

2.1.1. Design of Tracking Differentiator

According to reference[5],the general mathematical models for the discretized and continuous forms of the TD can be expressed as:

$$\begin{cases} Discretization\ TD: \begin{cases} fh = fhan\left(v_1 - v, v_2, r, h_0\right) \\ v_1\left(k+1\right) = v_1\left(k\right) + hv_2\left(k\right) \\ v_2\left(k+1\right) = v_2\left(k\right) + hfh \end{cases} \\ \text{Continualization } TD: \begin{cases} fh = fhan\left(v_1 - v, v_2, r, h_0\right) \\ \dot{v}_1 = v_2 \\ \dot{v}_2 = fh \end{cases} \end{cases} \tag{2}$$

where， r -speed factor; h-integration step size; h_0 -filtering factor; $\dot{v}_1$ 、 $\dot{v}_2$ -under the condition that $\dot{v}_1$ and $\dot{v}_2$ are differentiable,represent their respective first-order derivatives;

fh -steepest control synthesis function, whose expression is:

$$\begin{cases} d = rh_0 \\ d_0 = h_0 d \\ y_{\text{han}} = v_1 - v + h_0 v_2 \\ a_0 = \sqrt{d^2 + 8r\left|\mathrm{y}_{\text{han}}\right|} \\ a = \begin{cases} v_2 + \dfrac{\left(a_0 - d\right)}{2}\text{sign}\left(y_{han}\right), \left|\mathrm{y}_{\text{han}}\right| > d_0 \\ v_2 + y_{han}\left|h_0, \left|\mathrm{y}_{\text{han}}\right| \le d_0 \right. \end{cases} \\ fhan = -\begin{cases} \text{rsign}\left(a\right), \left|a\right| > d \\ \text{ra} / d, \left|a\right| \le d \end{cases} \end{cases} \tag{3}$$

2.1.2. Design of Extended State Observer

According to reference[5], the general mathematical models for the discretized and continuous forms of the ESO can be expressed as:

$$\begin{cases} \text{Discretization } ESO: \begin{cases} e(\mathrm{k}) = z_1(\mathrm{k}) - y(\mathrm{k}) \\ z_1(\mathrm{k}+1) = z_1(\mathrm{k}) + h\left[z_2(\mathrm{k}) - \beta_{01} e(\mathrm{k})\right] \\ z_2(\mathrm{k}+1) = z_2(\mathrm{k}) + h\left[z_3(\mathrm{k}) + f_0(\cdot) - \beta_{02}\, fal\left(e(\mathrm{k}), 0.5, \delta\right) + b_0 u\right] \\ z_3(\mathrm{k}+1) = z_3(\mathrm{k}) + h\left[-\beta_{03}\, fal\left(e(\mathrm{k}), 0.25, \delta\right)\right] \end{cases} \\ \text{Continualization } ESO: \begin{cases} e = z_1 - y \\ \dot{z}_1 = z_2 - \beta_{01} e \\ \dot{z}_2 = z_3 + f_0(\cdot) - \beta_{02}\, fal\left(e, 0.5, \delta\right) + b_0 u \\ \dot{z}_3 = -\beta_{03}\, fal\left(e, 0.25, \delta\right) \end{cases} \end{cases} \tag{4}$$

where， β_{01} 、 β_{02} 、 β_{03} -are coefficients to be determined; $\dot{z}_1$ 、 $\dot{z}_2$ 、 $\dot{z}_3$ -under the condition that z_1 、 z_2 、 z_3 are differentiable,represent their respective first-order derivatives; δ -is the length of the linear interval; $fal\left(e, 0.25, \delta\right)$ -is the nonlinear function.

2.1.3. Design of Extended State Observer

NLSEF generates the preliminary control quantity u_0 through a nonlinear combination of the errors between the transition process signals v_1 , v_2 provided by the Tracking Differentiator (TD) and the state estimates z_1 , z_2 provided by the Extended State Observer (ESO).

The state error e_1 and the error derivative e_2 are defined as follows:

$$\begin{cases} e_1 = v_1 - z_1 \\ e_2 = v_2 - z_2 \end{cases} \tag{5}$$

Where v_1 is the arranged transient process,and z_1 is the estimated value of the system output; v_2 is the derivative of the transient process,and z_2 is the estimated value of the output derivative.

Based on the above error signals and the fal function,the typical second-order system nonlinear PD control law (i.e., the output u_0 of the NLSEF) is designed as follows[6]:

$$u_0 = \beta_1 \mathrm{fal}\left(e_1, \alpha_1, \delta\right) + \beta_2 \mathrm{fal}\left(e_2, \alpha_2, \delta\right) \tag{6}$$

where β_1 and β_2 are the proportional gain and derivative gain,respectively.

Finally,combining the real-time estimate z_3 of the total disturbance (including internal dynamics and external disturbances) provided by the ESO,and according to the disturbance compensation principle,the final control quantity u acting on the controlled plant is:

$$u = \frac{u_0 - z_3}{b_0} \tag{7}$$

where b_0 is the control gain compensation factor of the system.By subtracting z_3, the system is reduced in form to an integrator series system,thereby achieving linearized control of the nonlinear and uncertain system.

3. DESIGN OF PMSM SPEED CONTROL SYSTEM BASED ON ACTIVE DISTURBANCE REJECTION CONTROL

The conventional double closed-loop vector control system for permanent magnet synchronous motors typically employs a speed regulator (ASR) and dq-axis current regulators (ACR) to implement feedback control of speed and current,respectively.However,the traditional PI controllers relied upon in this system exhibit inherent limitations,such as the difficulty in balancing fast dynamic response with overshoot suppression,and insufficient robustness against external disturbances and parameter variations.To address these issues,this paper investigates the application of Active Disturbance Rejection Control (ADRC) to enhance the speed control strategy.The specific scheme is illustrated in Fig.5,where the conventional PI controller in the speed loop is replaced by an ADRC controller.The detailed design process is described as follows:

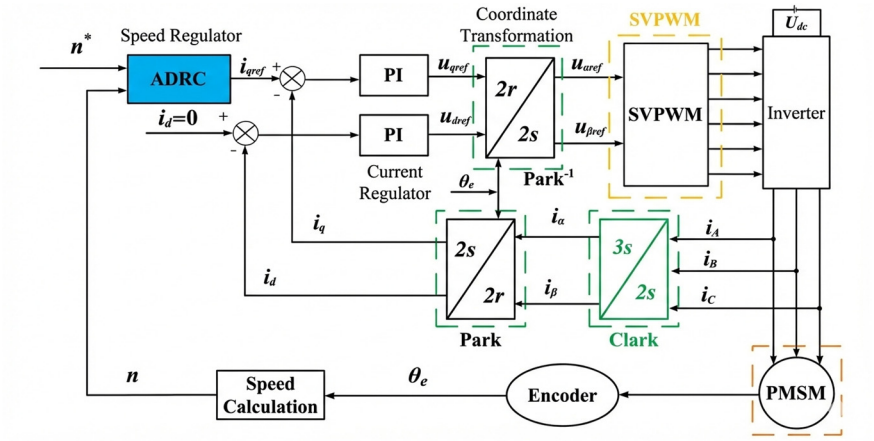

Fig 5. Vector Speed Control Strategy for PMSM Based on Active Disturbance Rejection Control

The speed regulator is controlled using NLADRC, and the structural block diagram of NLADRC is shown in Fig.6.

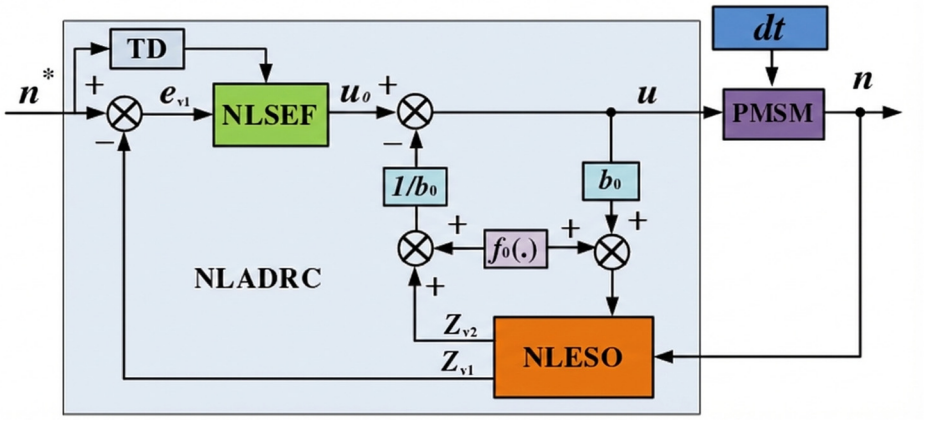

Fig 6. Structural Block Diagram of NLADRC

The selected permanent magnet synchronous motor (PMSM) is taken as the research object, and its specific parameters are shown in Table 1.

Table 1. Parameters of the Permanent Magnet Synchronous Motor

Parameter	Symbol	Value	Parameter	Symbol	Value
Stator resistance	R	$3.5\,\Omega$	damping coefficient	/	$1.5\times10\text{-}4\ N\cdot m\cdot s$
d-axis and q-axis inductance	$L_{\mathrm{d}}, L_{\mathrm{q}}$	$10.820\,mH$	number of pole pairs	P_{n}	8
flux linkage	φ_{f}	$0.128\,Wb$	DC bus voltage	V_{dc}	$311\,V$
moment of inertia	J	$0.9\,Kg\cdot cm^2$			

3.1. Stability Analysis of First-Order NLADRC Based on Lyapunov Method

This section addresses the first-order controlled plant of the PMSM speed loop,utilizing Lyapunov stability theory to demonstrate that the closed-loop system composed of the second-order NLESO and NLSEF possesses engineering stability.

Consider the first-order speed loop controlled plant model:

$$\dot{\omega}_m = f + b_0 i_q \tag{8}$$

To ensure the rigor of the proof, based on the physical characteristics of the actual system (the motor inertia and load cannot change instantaneously or become infinite),the following assumption is introduced:

Assumption (8):The total disturbance f of the system is differentiable,and its rate of change is bounded;i.e.,there exists a constant $D>0$ such that:

$$\left|\dot{f}\right| \le D \tag{9}$$

(1)Convergence Proof of Second-Order NLESO

For the second-order NLESO designed in Section 2.1.1,its dynamic equations are:

$$\begin{cases} e_1 = z_1 - \omega \\ \dot{z}_1 = z_2 - \beta_{01} g_1(e_1) + b_0 u \\ \dot{z}_2 = -\beta_{02} g_2(e_1) \end{cases} \tag{10}$$

where $g_i(e_1) = \mathrm{fal}(e_1, \alpha_i, \delta)$.Define the observation error variables as $\tilde{e}_1 = z_1 - \omega$ and $\tilde{e}_2 = z_2 - f$. Differentiating the error variables yields the error dynamic equations:

$$\begin{cases} \dot{\tilde{e}}_1 = \dot{z}_1 - \dot{\omega} = \left(z_2 - \beta_{01} g_1\left(\tilde{e}_1\right) + b_0 u \right) - \left(f + b_0 u \right) = \tilde{e}_2 - \beta_{01} g_1\left(\tilde{e}_1\right) \\ \dot{\tilde{e}}_2 = \dot{z}_2 - \dot{f} = -\beta_{02} g_2\left(\tilde{e}_1\right) - \dot{f} \end{cases} \tag{11}$$

Construct the Lyapunov candidate function V_o.

$$V_o\left(\tilde{e}_1, \tilde{e}_2\right) = \int_0^{\tilde{e}_1} \beta_{02} g_2(\tau)\, d\tau + \frac{1}{2}\tilde{e}_2^2 \tag{12}$$

Since the fal function is an odd function and monotonically increasing in the first and third quadrants,the integral term is always greater than or equal to zero; $\frac{1}{2}\tilde{e}_2^2 \ge 0$,therefore, V_o is positive definite.

Differentiating V_o along the error trajectory with respect to time yields:

$$\begin{aligned}\dot{V}_o &= \beta_{02} g_2(\tilde{e}_1)\dot{\tilde{e}}_1 + \tilde{e}_2\dot{\tilde{e}}_2 \\ &= \beta_{02} g_2(\tilde{e}_1)\left[\tilde{e}_2 - \beta_{01} g_1(\tilde{e}_1)\right] + \tilde{e}_2\left[-\beta_{02} g_2(\tilde{e}_1) - \dot{f}\right] \\ &= \beta_{02} g_2(\tilde{e}_1)\tilde{e}_2 - \beta_{01}\beta_{02} g_1(\tilde{e}_1) g_2(\tilde{e}_1) - \beta_{02} g_2(\tilde{e}_1)\tilde{e}_2 - \tilde{e}_2\dot{f} \\ &= -\beta_{01}\beta_{02} g_1(\tilde{e}_1) g_2(\tilde{e}_1) - \tilde{e}_2\dot{f} \end{aligned} \tag{13}$$

The first term, $-\beta_{01}\beta_{02} g_1(\tilde{e}_1) g_2(\tilde{e}_1)$,leverages the sign-preserving property of the fal function, where g_1 and g_2 share the same sign. Thus, this term is always negative (dissipative term). The second term, involving $\tilde{e}_2\dot{f}$, may be positive under the assumption that $|\dot{f}| \le D$.

Using inequality scaling:

$$\dot{V}_o \le -\beta_{01}\beta_{02}\left|g_1(\tilde{e}_1) g_2(\tilde{e}_1)\right| + |\tilde{e}_2| D \tag{14}$$

When the observation error is relatively large, the first term plays a dominant role,i.e., $\dot{V}_o < 0$,leading to energy dissipation and error reduction.When the error decreases to a certain neighborhood Ω such that the term $|\tilde{e}_2| D$ exceeds the dissipative term,the error no longer converges to zero but oscillates within this neighborhood.This demonstrates that the second-order NLESO is uniformly ultimately bounded stable.As long as the observer gain β is sufficiently large,this convergence neighborhood can be made sufficiently small to meet practical requirements.

(2) Stability Proof of the Closed-Loop System.

Under the premise that the ESO converges, we have $z_2 \approx f$. The control law is designed as:

$$u = \frac{u_0 - z_2}{b_0} \tag{15}$$

Substituting this into the original system $\dot{\omega} = f + b_0 u$, we obtain:

$$\dot{\omega} = f + (u_0 - z_2) = u_0 + (f - z_2) = u_0 - \tilde{e}_2 \tag{16}$$

At this point,the system is transformed into a perturbed integrator series system,where the disturbance term $-\tilde{e}_2$ is bounded.

A nonlinear P controller is adopted (for a first-order system, the NLSEF simplifies to a proportional element):

$$u_0 = k_p \mathrm{fal}(e_r, \alpha_c, \delta) \tag{17}$$

where the tracking error is defined as $e_r = v_1 - \omega$(with v_1 representing the target speed).Then, the closed-loop error equation is:

$$\dot{e}_r = \dot{v}_1 - \dot{\omega} = \dot{v}_1 - k_p \mathrm{fal}(e_r) + \tilde{e}_2 \tag{18}$$

Assuming that the target speed is constant ($\dot{v}_1 = 0$), construct the closed-loop Lyapunov function V_c :

$$V_c(e_r) = \frac{1}{2} e_r^2 \tag{19}$$

Differentiating with respect to time yields:

$$\dot{V}_c = e_r \dot{e}_r = e_r \left[-k_p \text{fal}\left(e_r\right) + \tilde{e}_2 \right] = -k_p e_r \text{fal}\left(e_r\right) + e_r \tilde{e}_2 \quad (20)$$

Similarly,the term $-k_p e_r \text{fal}\left(e_r\right)$ is always negative (stabilizing term).As long as the controller gain k_p is appropriately selected so that the feedback effect dominates the residual disturbance $\tilde{e}_2$,the overall $\dot{V}_c$ shows a negative definite trend.

The speed tracking error e_r of the first-order NLADRC closed-loop system is also uniformly ultimately bounded stable.The system is capable of maintaining the speed error within an acceptable accuracy range.

4. SIMULATION ANALYSIS OF PMSM SPEED CONTROL BASED ON NLADRC

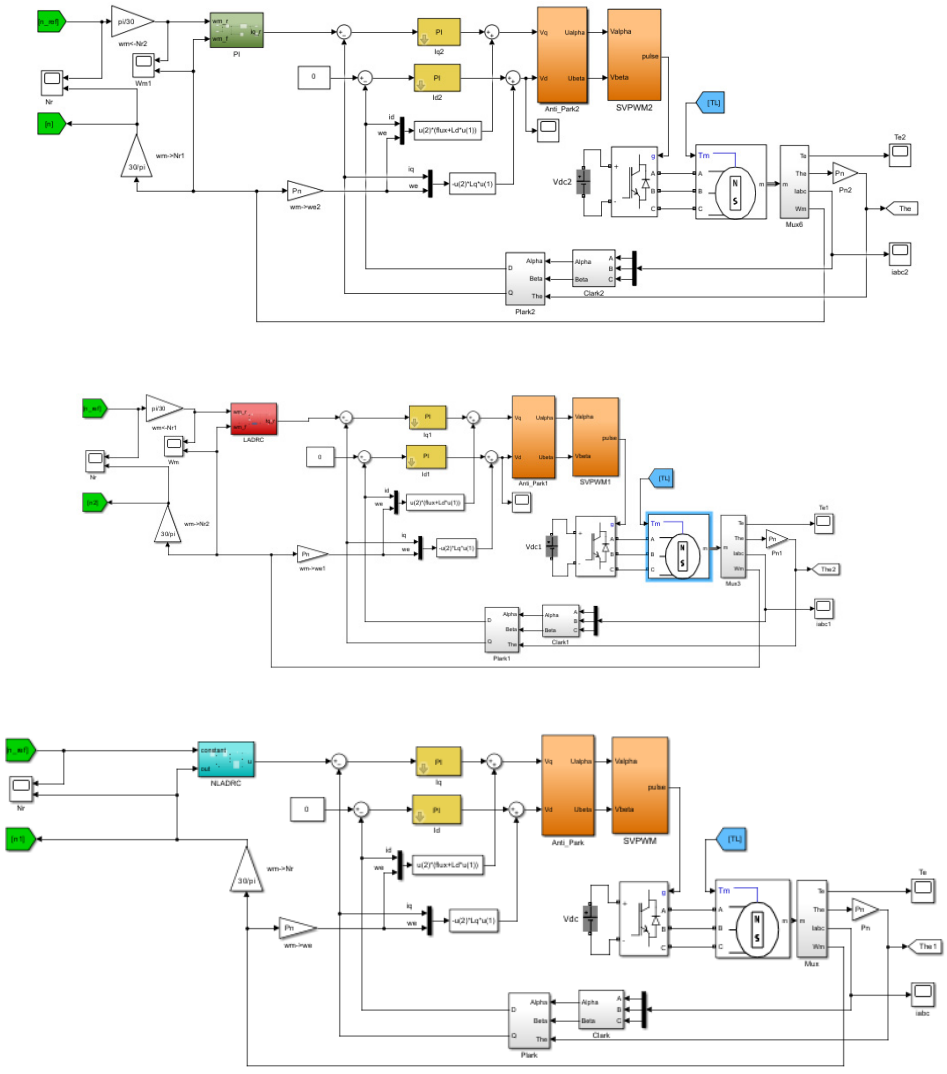

Fig 7. Simulation models of PMSM control systems based on NLADRC, LADRC, and PI control strategies

To comparatively analyze the advantages and disadvantages of the PMSM speed control strategies based on NLADRC and LADRC versus the vector control strategy based on a PI controller,

simulation comparison experiments are conducted using MATLAB/Simulink software. The simulation model of the PMSM control system based on Nonlinear Active Disturbance Rejection Control (NLADRC) is shown in Fig.7, where the current loop adopts traditional PI control. The PMSM parameters are taken from Table 2.

In this study, the no-load performance of the permanent magnet synchronous motor (PMSM) under three control strategies—NLADRC, LADRC, and PI—was simulated and analyzed. During the simulation, the reference speed of the motor was set to 3000 r/min, with a total simulation duration of 1 s. The motor started from a no-load state,a load torque of 2.33 N·m was applied at 0.3 s,and then removed at 0.6 s.The motor output response curves under the three control strategies are shown in Figures 8 and 9.

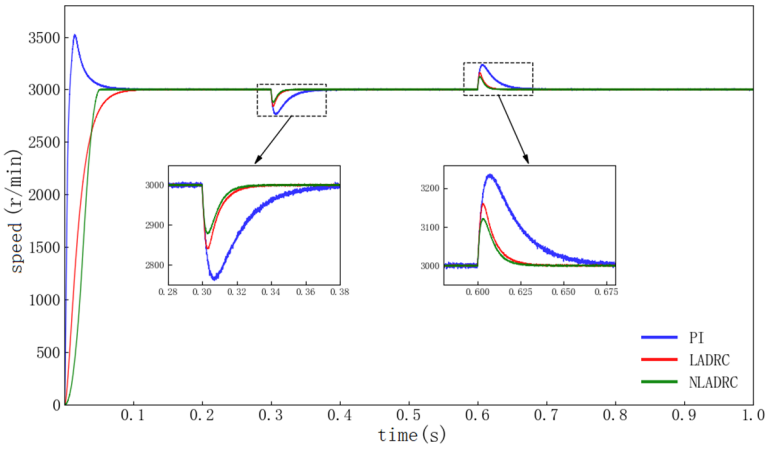

(a) Output Speed Diagram of PMSM Under Three Different Control Methods

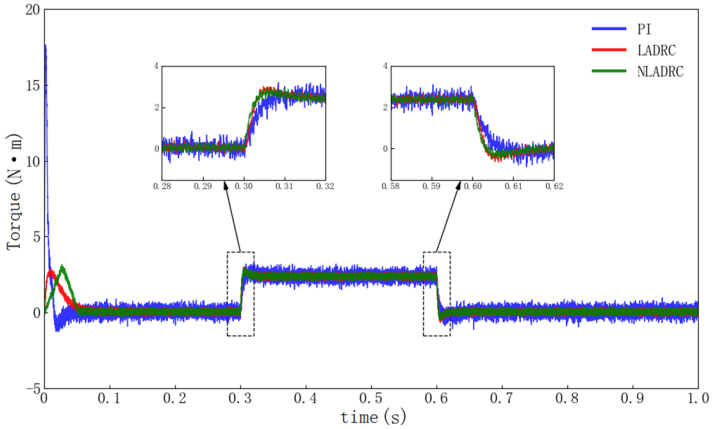

(b) Electromagnetic Torque Diagram of PMSM Under Three Different Control Methods

Fig 8. Output Response Curves of the Motor Under Three Control Strategies

In this study, the disturbance rejection performance of the three control strategies was quantitatively analyzed through simulation experiments on a PMSM speed control system. The data indicate the following:

From Fig.8(a),during the startup phase, the PI controller exhibits an overshoot of approximately 16%,whereas both LADRC and NLADRC achieve nearly 0% overshoot.Under rated load disturbances,the speed overshoot of the PI controller reaches 5%,which is unacceptable for high-precision servo applications.In contrast,LADRC limits the overshoot to within 2%,while NLADRC further reduces it to below 0.7%.This means that the dynamic accuracy of NLADRC is an order of magnitude higher than that of traditional PI control.Regarding recovery time,NLADRC achieves a recovery time of only about 12 ms,roughly 1/12 of that of the PI controller (150 ms).Although

LADRC has a simpler structure and outperforms PI,its convergence speed in the small-error region is inferior to that of NLADRC.The data demonstrate that the introduction of nonlinear functions enables large gain for small errors,providing stronger restorative force under minor disturbances and enabling nearly perfect overshoot-free performance during load shedding.

From Fig.8(b),the electromagnetic torque waveforms intuitively corroborate the performance differences among the control strategies: During startup,PI generates approximately 15% negative braking overshoot due to integrator saturation and delayed response,while NLADRC achieves smooth torque with zero overshoot owing to the transient planning of the TD.At 0.3 s during loading,PI can only build torque in a ramp manner (taking 100 ms with 20% overshoot),whereas NLADRC leverages ESO observation to achieve stepwise compensation within 10 ms (with overshoot less than 5%).At 0.6 s during load shedding,compared to the severe reverse impact exceeding 150% and prolonged oscillations exhibited by PI,NLADRC produces only minor adjustments of less than 10% and rapidly returns to zero within 15 ms.This conclusively demonstrates the overwhelming advantages of its active observation-feedforward compensation mechanism in addressing integrator saturation and enhancing dynamic stiffness.

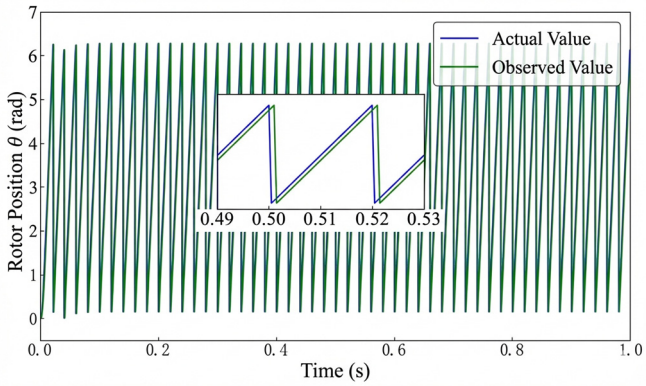

(a) Observed and Actual Values of Rotor Position Angle under NLADRC

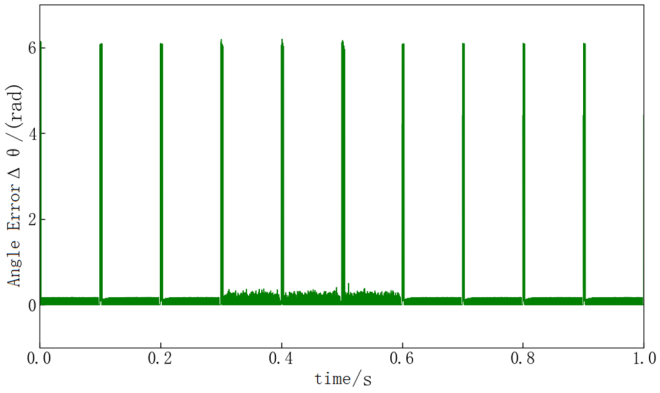

(b) Observation Error of Rotor Position Angle

Fig 9. Simulation Diagram of NLADRC Estimation

From the macroscopic response curves,it can be observed that after a brief transient process during the initial startup,the output state of the observer rapidly converges to the true state of the system.The periodic sawtooth waveform shown in Fig.9(a) indicates that the motor is in a stable high-speed rotation state.Throughout the entire simulation period, the observed angle curve and the actual angle curve exhibit a high degree of coincidence,almost perfectly overlapping.This demonstrates that the designed Extended State Observer (ESO) possesses excellent dynamic response speed,enabling real-time and accurate reconstruction of the rotor position signal without significant phase lag or amplitude attenuation.The locally enlarged view further reveals tracking details on a microscopic time scale.Even during rapid signal changes,the observation error is maintained within an extremely small

range.This indicates that the NLADRC algorithm can effectively cope with internal parameter perturbations and external disturbances, reflecting the strong robustness and anti-interference capability of this control strategy in position estimation.In summary, the simulation results validate the effectiveness of the NLADRC algorithm proposed in this paper for PMSM position observation.Its high-precision position estimation performance lays a solid foundation for subsequent high-performance sensorless control or closed-loop feedback control.From the observation results shown in Fig.9(b),it can be seen that there is a certain phase lag in the observed values relative to the actual values.This lag,during the conversion between angle and radian units,causes an angular jump close to 2π in each electrical cycle (a phenomenon that is part of the system's normal response).

5. SUMMARY

To address the issues of insufficient disturbance rejection capability and sluggish dynamic response in current permanent magnet synchronous motor speed control systems, this paper proposes two vector speed control strategies based on active disturbance rejection control theory.To validate the effectiveness of the proposed control methods,corresponding simulation models are established in the MATLAB/Simulink platform,and systematic simulation experiments are conducted through appropriate selection of controller parameters.The main work accomplished in this paper is as follows:Speed control strategies for permanent magnet synchronous motors based on LADRC and NLADRC are designed.The stability of the designed controllers is analyzed and proved using Lyapunov functions.Simulation models for the LADRC-based and NLADRC-based PMSM speed control strategies are built in MATLAB/Simulink.Through simulation experiments,it is verified that the NLADRC-based control strategy exhibits superior control performance in terms of tracking characteristics,response characteristics,and disturbance rejection capability.

REFERENCES

[1] Zuo Y, Mei J, Jiang C, et al. Linear Active Disturbance Rejection Controllers for PMSM Speed Regulation System Considering the Speed Filter. IEEE Transactions on Power Electronics. 2022, Vol. 37 (No. 4), p.4108-4121.

[2] Qu L, Qiao W, Qu L, et al. Active-Disturbance-Rejection-Based Sliding-Mode Current Control for Permanent-Magnet Synchronous Motors.2020 IEEE Energy Conversion Congress and Exposition (ECCE). Detroit, USA, Oct.11-15 2020, p.3206-3211.

[3] Wang G, Valla M I, Solsona J, et al. Advanced Control Systems for Electric Drives. Springer, 2022, p.115-130.

[4] Li H, et al. Design of Unmanned Helicopter Distributed Electric Tail Rotor Controller Based on Improved Active Disturbance Rejection Control. IEEE Access.2024, Vol.12, p.97053-97066.

[5] Ali Z, et al. ADRC Parameters Tuning Using Traditional and AI-Based Methods: A Survey. IEEE Access.2024, Vol. 12, p.5150-5175.

[6] Qu L: Active Disturbance Rejection Control for Permanent-magnet Synchronous Motor Drives (Ph.D., University of Nebraska, USA 2021). p.25-30.